STRENGTH OF A COHESIVE SOIL IN IRREGULAR LOADING

K. Ishihara (I)
N. Koyamachi (II)
K. Kasuda (III)
Presenting Author: K. Ishihara

SUMMARY

Several series of dynamic triaxial tests were conducted on a partially saturated sandy clay by employing four different time histories in the stroke of the axial load. The test results were summarized in a form of shear stress versus residual strain relationship in which the peak in dynamic load time history plus the sustained static shear stress is plotted versus the amount of residual component of shear strain. The test results showed that, when failure condition is expressed in terms of the Mohr-Coulomb type criterion, the cohesion component in the dynamic loading increases well over the value of cohesion obtained in the static loading test, whereas the angle of internal friction remains unchanged whether the loading is dynamic or static.

INTRODUCTION

A conventional method of approach to evaluate the stability of slopes during earthquakes has been the so-called pseudo-static method in which the effect of an earthquake-induced inertia force is taken into account by an equivalent static force determined as the product of a seismic coefficient and the weight of the potential sliding mass. While the issue of the seismic coefficient has been a focus of exhaustive discussions in recent years, the aspect of soil resistance to be incorporated into the analysis has been left almost unheeded and seldom been the subject of careful consideration.

One of the ideas for a proper choice of the seismic coefficient would be to take up a value corresponding to a peak ground acceleration expected to occur at a site in question. When such a seismic coefficient is to be used in the pseudo-static method of analysis, the appropriate soil strength must be determined under irregular loading conditions simulating the actual load variation during an earthquake, and the soil strength should be expressed in terms of the maximum shear stress corresponding to the peak in the time history of acceleration. In view of the need for the soil strength in such analysis procedures, some efforts have been made to test soil specimens under irregular loading conditions (Ishihara and Nagao, 1981 ; Ishihara et al, 1983). In the present paper, some of the results of tests conducted in similar vein on the other type of cohesive soils

(I) Professor of Civil Engineering, University of Tokyo, Tokyo, Japan

(II) Civil Engineer, Fudo Construction Co. Tokyo, Japan

(III) Graduate Student of Civil Engineering, University of Tokyo, Tokyo, Japan

are described.

TEST EQUIPMENT AND MATERIALS

A conventional triaxial shear test apparatus was incorporated into an electro-hydraulic servo loading system by which any desired form of axial load history can be produced and applied to test specimens. Irregular time histories stored in a tape recorder were retrieved and transmitted to the actuator to reproduce controlled motions in the triaxial loading piston (Ishihara-Yasuda, 1972).

Disturbed samples of a volcanic sandy clay were procured from a site of man-made fills which had suffered a large-scale landslide at the time of the 1978 June 12 Miyagiken-oki earthquake (M=7.4). The slide area is located at Kotobukiyama in the suburb of Shiroishi city about 75 km southwest of Sendai. The soil from valcanic origin consists of a mixture of 13 % of gravel, 47 % of sand, 12 % of silt and 28 % of clay content. The specific gravity is 2.575, and liquid limit and plasticity index of this soil are 41 % and 18 %, respectively. The specimens for the laboratory tests were prepared by compacting the material to a density representative of that in-situ. The material was compacted in a standard model (1000 cm^3 in volume) by placing moist soil in three layers and by tamping 25 times for each layer by means of a drop hammer of 2.5 kgf. The specimens thus prepared had a water content of 22 ~ 23 % with a saturation ratio of about 84 %. The specimens compacted in the mold were taken out and trimmed so as to have a diameter of 5 cm and a length of 10 cm. The cohesion and angle of internal friction of this soil specimen determined from the result of the conventional triaxial test were 28 kN/m^2 and 14°, respectively.

DYNAMIC LOADING SCHEME

The entire loading scheme adopted in the present study is illustrated in Fig. 1. A specimen is first consolidated under a confining pressure, σ_0', as in the static test and then subjected to an initial axial stress, σ_s, under drained conditions. A sequence of an irregular axial load is applied to the test specimen with a relatively small amplitude. In the course of this phase of loading, the specimen deforms to a certain magnitude of residual strain, as designated for example by point B' in Fig. 1. The load with the same time history is again applied to the same test specimen with an increased amplitude. The specimen deforms further to a residual strain indicated by point B" in the schematic diagram of Fig. 1. Similarly, several sequences of the same irregular load are applied to the same specimen with amplitudes being stepwise increased in each sequence. When the points of the peak axial stress and residual strain such as C', C" and C'" are connected, it becomes possible to obtain a curve such as the dashed curve shown in Fig. 1. This curve may be deemed as representing the stress-residual strain relationship of soils under a given set of initial stear stress and irregular load conditions. In this type of loading sheme irregular loads with stepwise increasing amplitudes are applied to a single specimen in sequence. Therefore, it has an advantage that a stress-residual strain relation can be obtained using a single test specimen.

IRREGULAR WAVE FORMS USED IN THE TESTS

The irregular load pattern used in the present tests are four series of time histories of the horizontal accelerations that were obtained on the surface of medium dense sand deposits at Hachinohe and Muroran harbors at the time of the Tokachioke earthquake of 1968. These time histories are shown in Fig. 2. The acceleration time history of the EW-component at Muroran is shown in Fig. 3(a). All these wave forms except the EW of Hachinohe have a few predominant peaks and are classified accordingly as the shock type wave (1). The EW-component at Hachinohe has several large spikes and is classified as the vibration type wave form. Both types of wave forms are assumed as representative of the irregular load pattern to which the ground consisting of relatively stiff materials is subjected during earthquakes.

TEST PERFORMANCE

In the complicated history of stress change, it is always possible to locate a spike where a maximum shear stress occurs. When this stress change is transferred to a specimen by the up-and-down movement of the triaxial loading piston, one of the loading modes is to orient the stress time change so that the peak can be attained when the piston reaches the lowest position. This type of test will be referred to as CM-test (1). It is also possible to have the peak stress oriented so that the peak is executed at the highest position of the loading piston. This type of test will be referred to as EM-test. For each of the wave forms used, both types of test were performed in the present investigation.

One of the results of such series of tests is shown in Fig. 3. The test is of the CM-type. The static strength, σ_f, defined as the axial stress causing failure in the statically performed monotonic loading test was 100 kN/m^2 for the test specimens subjected to a confining pressure of $\sigma_0' = 50$ kN/m^2. The initial axial stress, σ_s, 60 % of the static strength was used throughout this test program. Fig. 3(a) shows the time history of the EW-component of the acceleration obtained at Muroran which was converted to the axial stress in the triaxial test apparatus. Fig. 3(b) shows the time change of axial strain recorded in the first test sequence where the amplitude of peak axial stress was 39 kN/m^2 in the direction of triaxial compression. It is observed that the residual axial strain produced in the specimen by the application of the irregular load was $\varepsilon_r = 0.15$ % in this first sequence. Prior to executing this loading sequence, the test specimen had already sustained a residual strain of $\varepsilon''_{re} = 3.21$ % during the initial static phase of loading, as accordingly indicated in Fig. 3(b). Fig. 3(c) shows the time change of the axial strain recorded in the subsequent test sequence in which the amplitude of the irregular load was raised to $\sigma_d = 60$ kN/m^2. The specimen having undergone a parmanent axial strain of $\varepsilon'_{re} = 3.36$ % until the preceding sequence experienced an additional residual strain of $\varepsilon_r = 1.81$ % in the course of the second loading sequence. Skipping two intermediate sequences, the result of the last test sequence is demonstrated in Fig. 3(d) where it is seen that the specimen underwent a re-

sidual axial strain as large as 4.06 %.

An example of similar test sequences employing a reversely oriented wave form (EM-test) is presented in Fig. 4. The specimen used in this test showed approximately the same static strength of σ_f = 100 kN/m^2 under the confining pressure of σ_0' = 50 kN/m^2. The time changes in the axial strain shown in Figs. 4(b), (c) and (d), are construed in the same context as in the case of the results of the CM-test shown in Fig. 3. It should be noted that the amplitude of the peak, σ_d, indicated in Fig. 4 refers to the maximum spike on the side of triaxial compression. In the type of triaxial test procedures employed in the present study, the initial axial stress, σ_s, is applied towards the triaxial compression side, and therefore the key phenomena such as residual strains and failure of test specimens are always induced on the side of triaxial compression. Accordingly, it is deemed reasonable to take up the peak stress on the triaxial compression side as a key variable influencing the development of the residual strains and failure of the specimen.

TEST RESULTS

The time histories of the recorded axial strains shown in Fig. 3 and 4 indicate that major part of the residual strains is produced when the peak axial stress is applied to the specimen, and the irregular load after the advent of the peak exerts virtually no influence on the development of additional residual strain. This appears to imply that large displacements or failure produced in clay slopes during earthquakes take place almost at the same time as the peak shear stress is applied to soil elements in the field.

In order to establish the stress-residual strain relationships as illustrated in Fig. 1, values of the total residual strain, $\varepsilon'_{re} + \varepsilon_{re}$, accumulated up to the current sequence of irregular loading tests were read off from the test records such as those shown in Fig. 3 and 4, and these values were plotted versus the peak amplitude of the current irregular loading, σ_d, plus the initial axial stress, σ_s. Note that the peak amplitude, σ_d, plotted, refers to the peak on the triaxial compression side. The results of such data compilation for the cases of the tests shown in Fig. 3 and 4 are presented in Fig. 5. In this plot, the combined static and dynamic axial stress, $\sigma_s + \sigma_d$ is shown normalized to the static strength, σ_f, in order to discern the effect of dynamic loading as against the static behavior. In Fig. 5 the data points indicated by arrows are those which were read off directly from the test results shown in Figs. 3 and 4. It may be seen in Fig. 5 that there is some difference in the stress-residual strain relationship between the CM- and EM-tests, but overall both test results give a consistent trend. Also indicated in Fig. 5 are the stress-strain curves for the static phase of loading until the initial shear stress, σ_s, is increased to 60 % of the static strength. The static stress-strain curves which would have been obtained if the loading had been continued further up are shown in Fig. 5 by dashed lines. It may be seen in Fig. 5 that the stress-strain curve for the static-dynamic loading is located far above the stress-strain curve for the static loading alone. This fact indicates that if the soil specimen is subjected to a dynamic load after it has deformed statically to some extent, the specimen tends to show a larger stiffness and higher strength than it is loaded to failure all the

way in static conditions. For a volcanic clay soil as tested in the present study, the increase in strength in the dynamic loading over that in the static loading condition amounts to almost 60 % as indicated in Fig. 5. Such an increase in soil strength appears to emerge from highly rate-dependent nature of fine-grained portion of the tested soil when subjected to rapid loads such as those used in the present test scheme. This aspect of the problem is discussed more in detail elsewhere (2).

Results of tests employing other load time histories are presented in Fig. 6 together with the test results shown in Fig. 5. Although there exist some scatters depending upon the kind of time histories and their orientation (CM or EM), all data points fall in a relatively narrow zone enclosed by dashed lines in Fig. 6. A reasonable average curve is, therefore, drawn through the entire set of data. It may be seen in Fig. 6 that the axial stress required to cause failure strain, say, 15 % is about 1.6 times as much as the strength achieved under the static loading conditions

DISCUSSIONS OF TEST RESULTS

As mentioned in the foregoing section, one of the important conclusions drawn from the previous test scheme (Ishihara et al, 1983) was that the stress-residual strain relationship is not appreciably affected by the initial shear stress, if its value stays within the range of σ_s/σ_f = 0.5 and 0.8, which is generally the case with stress conditions in in-situ deposits of soils under slopes. On the other hand, effects of the confining stress were shown to be remarkable and can not be disregarded in evaluating the stress-residual strain relationship of cohesive soils. Therefore, it was considered necessary in this study to investigate into the influence of the confining stress. To this end, two more series of tests were carried out on identically prepared specimens of the same soil by employing confining pressures of 80 and 100 kN/m^2. In each series of the tests, specimens were consolidated under a specified confining stress and then subjected, under drained conditions, to the initial axial stress equal to 60 % of the static strength. The dynamic tests employing the four time histories were then carried out. All test results in each series were plotted together in the same manner as was done in Fig. 6 for the case of σ_0' = 50 kN/m^2. Then, a reasonable average curve was drawn through the entire set of test data to establish a stress-residual strain relationship. The curves thus determined are assembled and shown together in Fig. 7.

In order to put the effects of confining stress in a proper perspective, let the dynamic strength be represented in the form of Mohr circle in the stress space as in the case of the static strength representation. The method of establishing a Mohr-Coulomb type failure criterion is illustrated in Fig. 8. The value of the confining stress, σ_0', is first laid off at point A in abscissa and then the static and dynamic strength values are laid off towards the right as AB and AC, respectively. A circle drawn through points A and B is the Mohr circle associated with failure in the static loading. Likewise, the Mohr circle for failure in the dynamic loading can be constructed by drawning a circle through points A and C.

Using the above procedures, a pair of Mohr circles specifying failure in static and dynamic loading conditions were established for the test data on sandy clay shown in Fig. 7. The Mohr circles and straight-line envelops

are shown in Fig. 9. It can be seen in this figure that for the sandy clay from Shiroishi compacted to a dry density of about 15.2 kN/m^3, the cohesion component for static loading, C, was 28 kN/m^2 and the cohesion component for dynamic loading, C_d, was 52 kN/m^2. It is to be noted that the angle of internal friction is practically the same both for the static and dynamic loading conditions. The angle of internal friction, ϕ, for the sandy clay tested was 14°. The fact that the effects of dynamic loading is manifested only through the cohesion component whereby keeping the frictional angle unchanged is coincident with the findings obtained in the previous test scheme which was executed on a volcanic clay from Isu Peninsula (Ishihara et al, 1983). According to the results of the previous that scheme, the increase of cohesion component in dynamic loading over the cohesion in static loading was 2.4 times for the volcanic clay having a plasticity index of PI = 30. Since the increase of cohesion in dynamic loading appears to emerge from the viscous nature of cohesive soils, it may be of interest to examine the rate of increase of dynamic cohesion over the static cohesion in the light of the plasticity index of the soils tested. In view of the fact that the rate of cohesion increase was $C_d/C = 1.86$ for the sandy clay from Shiroishi having a plasticity index of about 18, it may well be mentioned that a soil material with higher plasticity index exhibits a higher rate of increase of cohesion in dynamic loading as compared to the rate of cohesion increase exhibited by a soil with lower plasticity index.

CONCLUSION

The results of several series of dynamic triaxial tests conducted on a partially saturated compacted sandy clay by employing four different time histories in the stroke of the axial load disclosed that while the angle of internal friction remains practically the same for both static and dynamic loading, the cohesion component specifying failure in the dynamic loading is increased about 1.86 times over the cohesion component in the static loading. In the light of the results of similar tests performed previously on a volcanic clay, it was suggested that a cohesive soil with higher plasticity index tends to exhibit an higher rate of cohesion increase in dynamic loading than does a soil with lower plasticity index.

REFERENCES

(1) Ishihara, K. and Yasuda, S. (1972), "Sand Liquefaction due to Irregular Excitation," Soils and Foundations, Vol.12, No.4, pp.65-77.

(2) Ishihara, K and Nagao, A. (1981), "Strength of Weathered Tuff under Irregular Dynamic Loading Conditions," Proc. International Symposium on Weak Rock, Tokyo, Vol.2, Balkema, pp.1217-1222.

(3) Ishihara, K., Nagao, A. and Mano, R. (1983), "Residual Strain and Strength of Clay under Seismic Loading," Proc. 4th Canadian Conterence on Earthquake Engineering, pp.602-613.

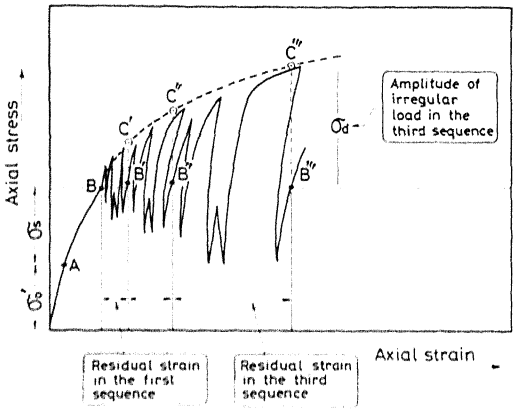

Fig. 1 Loading scheme used in the tests

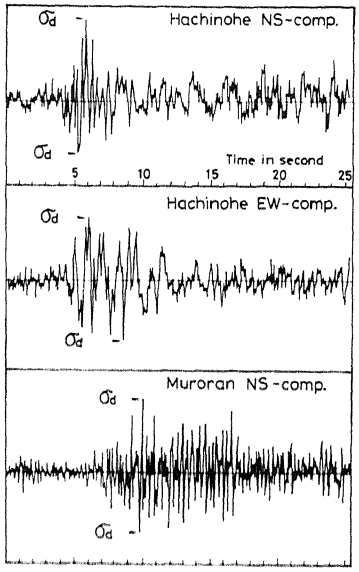

Fig. 2 Irregular time histories of loads used in the tests

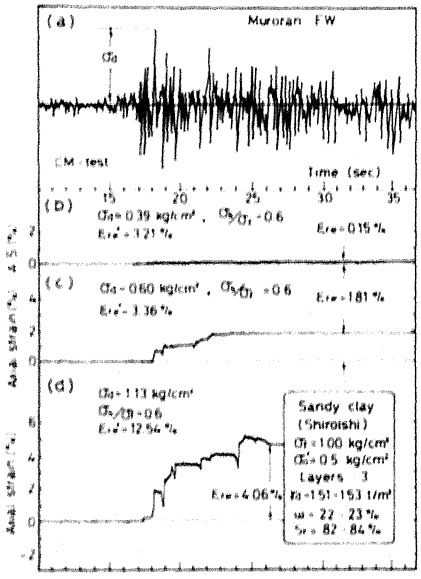

Fig. 3 Evolvement of residual strains in the irregular loading test (CM-test)

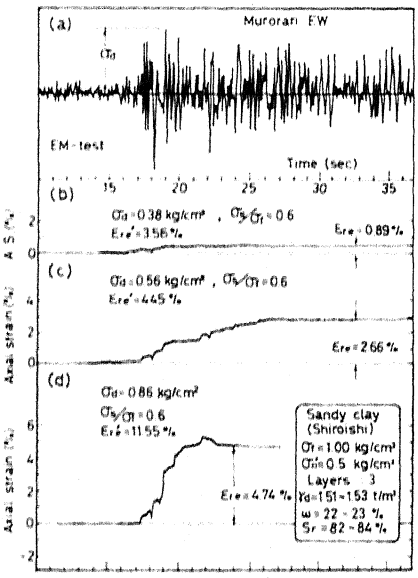

Fig. 4 Evolevment of residual strians in the irregular loading test (EM-test)

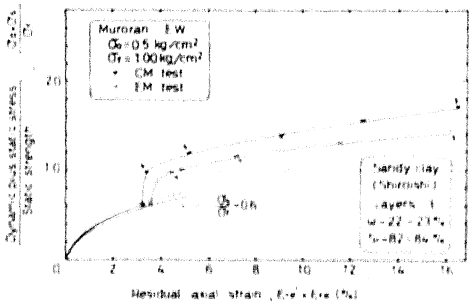

Fig. 5 Shear stress-residual strain relationships

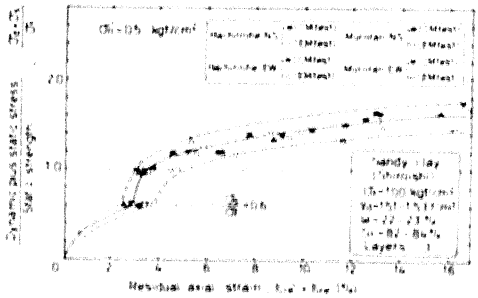

Fig. 6 Shear stress-residual strain relationships for different irregular loads

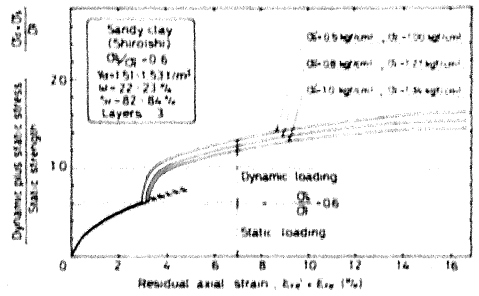

Fig. 7 Summary of stress-residual strain relationships for different confining stresses

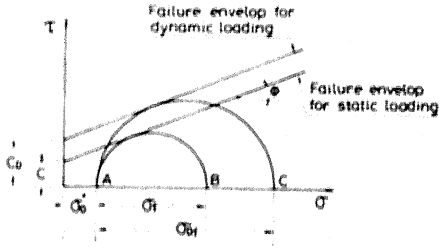

Fig. 8 Construction of Mohr circles and failure envelops associated with static and dynamic loading

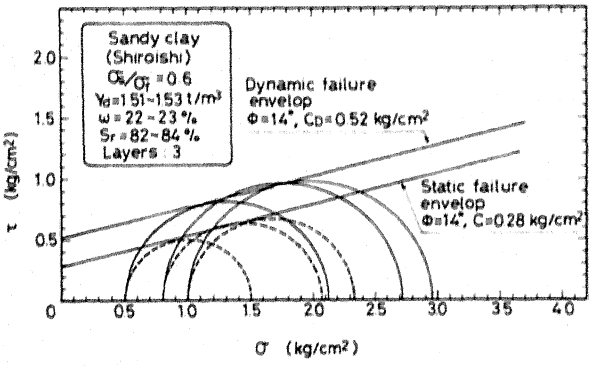

9 Failure envelops obtained from static and dynamic loading test results